Effect of Mn substitution on structural and magnetic properties of cobalt ferrite

Swati Tapdiya*, Ashwani K. Shrivastava, Sarika Singh

SoS in Physics, Jiwaji University, City Center, Gwalior, 474011, India

*Corresponding author; Tel. (+91) 7828596649; E-mail: swati.phy@rediffmail.com

Received: 31 March 2016, Revised: 30 September 2016 and Accepted: 20 April 2017

DOI: 10.5185/amp.2017/695
www.vbripress.com/amp

Abstract

Manganese substituted Cobalt Ferrite $Co_{1-x}Mn_xFe_2O_4$($0.0 \le x \le 0.3$) nanoparticles were prepared using low temperature chemical co-precipitation method. All the samples were annealed at 900°C for 3 hours. The crystal lattice symmetry and phase purity were performed by X-ray diffraction (XRD). The varying dopent concentration affects the crystalline size, surface morphology and magnetic properties of the cobalt ferrite. The particle sizes are found to be in the range of 29-37 nm. SEM with EDAX examines the morphological and compositional analysis of the nanoparticles. EDAX confirms the presence of Co, Mn, Fe and O. Fourier transform infrared spectroscopy (FTIR) study confirms the formation of spinel ferrite. The saturation magnetization, magnetic remanence and coercive field of CoMn nanoparticles are obtained at room temperature. Saturation magnetization initially increases and then decreases for higher value of dopent, which shows applicability of these materials for recording media and magnetic data storage. Copyright © 2017 VBRI Press.

Keywords: Cobalt ferrite, nanoparticles, x-ray diffraction, SEM, saturation magnetization.

Introduction

Spinel ferrites have been under intense research for the past five decades due to their countless applications such as magneto-optic recording material, microwave industries, gas sensors solar cells and drug delivery [**1-5**]. Mixed metal oxide with iron (III) oxide as their main components are technologically very important class of magnetic oxides because of their high electrical resistivity, good magnetic properties [**6**]. Cobalt ferrite has a cubic close-packed fcc like lattice of oxygen ions, are described by the formula $(A)[B]_2O_4$, where (A) and [B] represent tetrahedral and octahedral sites, respectively. The Co^{2+} and Fe^{3+} ions occupy one of the two interstitial sites -tetrahedral (A) or octahedral (B) sites. In the ideal inverse spinel $CoFe_2O_4$, the A-sites must completely be occupied by Fe^{3+} ions and the B-sites must randomly be occupied by the remaining Fe^{3+} ions together with the Co^{2+} ions. Magnetic properties of cobalt ferrite materials can be enhanced by doping of different elements. Mn^{2+} ions posses' large magnetic moment (5μB) can alter the magnetic properties of cobalt ferrite [**7**].

Ferrite particles in nano scales can be produced by soft chemical methods such as co-precipitation [**8**], sol-gel [**9**], ceramic method [**10**] and hydrothermal synthesis [**11**]. Among these methods, the co-precipitation has been chosen in the present study as the conditions of synthesis in this method are highly controllable and further it provides homogeneous powders of highest yield at temperatures close to 100°C.

Experimental

Materials

AR grade Manganese Chloride 98% (CDH Ltd.) Cobalt Chloride 98% (Sigma-Aldrich) ($CoCl_2.6H_2O$,) and Ferric Chloride 99.9% (Sigma –Aldrich) used as starting materials. Sodium hydroxide (NaOH) used as precipitating agent. Acetone were used for washing of samples. All the Chemicals used in present investigation are used without further purification. Double distilled water was used as solvent.

Material synthesis

A series of manganese doped cobalt ferrite samples with composition of $Co_{1-x}Mn_xFe_2O_4$ ($0.0 \le x \le 0.3$) were prepared by substituting manganese for cobalt by chemical co precipitation method. Aqueous solution of 0.2M Cobalt Chloride ($CoCl_2.6H_2O$), Manganese Chloride ($MnCl_2.4H_2O$) and 0.4M Ferric Chloride ($FeCl_3$) were taken in stoichiometric ratio. All the constituents were dissolved in 25ml distilled water individually and the solutions were mixed together in the same vessel. Sodium hydroxide (NaOH) was used as precipitating agent. The pH of solution Maintained at 10-11 using drop wise addition of NaOH into mixture solution with rigorous stirring at room temperature. The solutions were then kept at apparatus at 90-95°C for 1 hour in constant temperature water bath apparatus. At this temperature co precipitation reaction takes place and desired CoMn Nanoparticles formed. The solutions then cool down at

room temperature after completing reaction. The final product was washed several times with distilled water and acetone to remove any organic or inorganic impurities. The solutions were then centrifuge for 15 min at 4500 rpm and dried overnight at 100ºC. The dried samples were then ground into fine powder and annealed at 900ºC for 3 hrs to obtain pure CoMn ferrite nanoparticles [**12**].

Characterizations

Manganese doped cobalt ferrite $Co_{1-x}Mn_xFe_2O_4$ ($0.0 \le x \le 0.3$) samples were subjected to XRD analysis with Bruker D8 Advance X-ray diffraction unit (Cu-Kα radiation λ=1.5418 Å) to explore the structural properties. The scanning electron microscope was used to examine the particle morphology using a LEO 435 VP scanning electron microscope (SEM) along with the energy dispersive X-ray analysis (EDX). The magnetic properties of the samples were investigated using vibrating sample magnetometer (VSM) Lakeshore VSM 7410. To confirm presence of functional group FTIR spectrum was recorded using Perkin-Elmer spectrum using KBr pallet technique.

Results and discussion

The XRD pattern of powder samples of CoMn ferrite is represented in **Fig. 1.1** confirms the formation of single phase cubic spinel structure. The major peaks could be indexed as (220), (311), (400), (422), (511) and (440) which are characteristics of a cubic spinel structure. The obtained diffraction peaks are well matched with the standards JCPDS card No.22-1086 for $CoFe_2O_4$ [**13**].

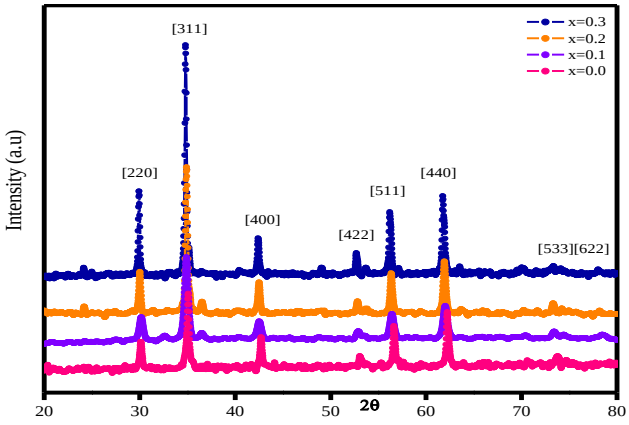

Fig. 1.1 XRD spectra of Mn doped Cobalt ferrite nanoparticles for $0.0 \le x \le 0.3$

Structural parameters including crystallite size, lattice parameter, X-ray density, bulk density and interatomic distances at A-A and B-B site were calculated from XRD pattern are shown in **Fig. 1.2** and **Table 1.1**. The intensity of the strongest diffraction peak at the plane (311) was considered as a measure of its degree of crystallinity. The average crystallite size (D) of all the samples was calculated by using the Scherer's formula [**14**]:

$$D = \frac{0.9\lambda}{\beta\cos\theta} \quad \text{.....(1)}$$

where, λ is the wavelength of Cu-Kα (1.54Å) radiation used, β and θ is full width at half maximum (FWHM) and angle of strongest intensity peak respectively. Crystal size found to be in the range 29-37 nm which is in good agreement with results reported by A.B. Salunkhe et *al.*[**15**].

Lattice constant 'a' was determined from the miller indices (hkl) using relation [**6**]:

$$a = d_{hkl}\sqrt{h^2+k^2+l^2} \quad \text{.....(2)}$$

where, d is inteplaner spacing calculated from Bragg's law. It is observed that as Mn^{2+} content increases lattice parameter increases from 8.3676Å to 8.44 Å. This linear increase in lattice cons.(a) with Mn^{2+} content 'x' can be explained on the basis of difference in ionic radii of Co^{2+} (0.72Å), Fe^{3+}(0.64Å) and Mn^{2+}(0.83Å). The smaller ionic radius of Co^{2+} ions are replaced by larger Mn^{2+} ions as a consequence unit cell dimension expands which results in increase in lattice parameter. The doping of large sized ions Mn^{2+} into spinel type of structure of cobalt ferrite induces uniform strain in the lattice. Due to this effect lattice plane spacing changes and diffraction peaks shifted towards lower 2θ angles. The interatomic distance (hopping lengths) between magnetic ions at tetrahedral A (L_A) and octahedral B (L_B) sites was calculated by using the following relations [**11**]:

$$L_A = a\frac{\sqrt{3}}{4}, L_B = a\frac{\sqrt{2}}{4} \quad \text{.....(3)}$$

It is clear that as Mn^{2+} concentration increases hopping length also increases [**16**]. The X-ray density of all prepared nanoparticles was calculated using the relation [**17**]:

$$d_x = \frac{8M}{Na^3} \quad \text{.....(4)}$$

where, M is molecular weight, N the Avogadro number and 'a' is the lattice parameter.

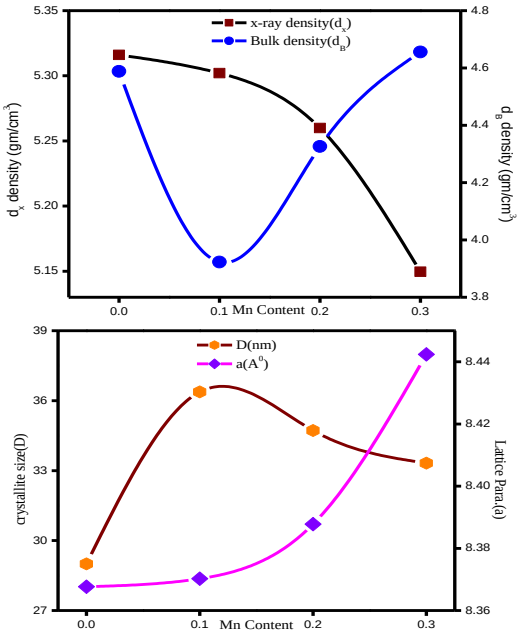

Fig. 1.2 Variation of structural parameters of Mn doped cobalt ferrite nanoparticles.

Table 1.1 Structural and magnetic parameters of $Co_{1-x}Mn_xFe_2O_4$() nanoaprticles annealed at 900ºC.

Parameters	x=0.0	x=0.1	x=0.2	x=0.3
D(nm)	29	37	34	33
a(Å)	8.367	8.3709	8.387	8.44
d_x(gm/cm^3)	5.314	5.309	5.259	5.149
d_B(gm/cm^3)	4.58	3.92	4.326	4.65
L_A(Å)	3.623	3.627	3.631	3.65
L_B(Å)	2.95	2.96	2.966	2.983
Ms(emu/g)	50.16	54.1	57.04	43.33
Hc(Gauss)	883	424	314	388
K_1(erg/cm^3)*10^4	4.6	2.4	1.9	1.7
nB(μB)	2.10	2.27	2.38	1.81

The Scanning electron micrograph of $Co_{0.9}Mn_{0.1}Fe_2O_4$ nanoparticles is shown in **Fig. 1.3**. It is clear from SEM images that particles agglomeration is uniform. The EDX analysis gives the qualitative composition of CoMn nanoparticles and also indicates the quantitative presence of Co, Mn, Fe, and O in the samples. It is clear that no extra impurities are present in our samples and the compositional molar ratio of (Co+Mn)/ Fe was close to 0.5.

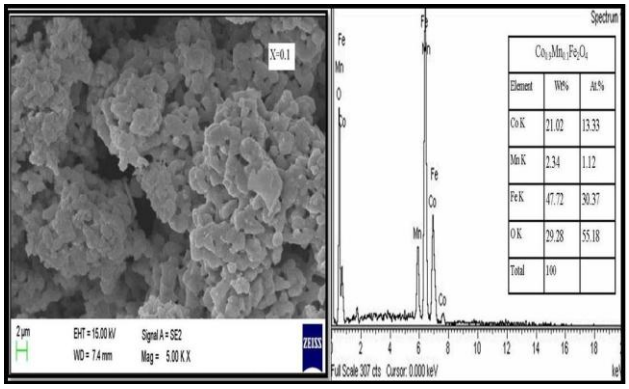

Fig. 1.3 SEM micrograph and compositional study of $Co_{0.9}Mn_{0.1}Fe_2O_4$ nanoaprticles.

Fourier transform infrared spectra (FT-IR) of $Co_{0.9}Mn_{0.1}Fe_2O_4$ was recorded in the range 4000 to 400 cm^{-1} is shown in **Fig. 1.4**. Stretching and bending of bonds at tetrahedral and octahedral sites are noticed. The broad peak observed at ~3670 cm^{-1} is coresponds to hydroxide (O–H) ions**[18]**.The peaks at ~1605cm^{-1} are assigned to H–O–H bending vibration in water molecule [**19**] or OH deformation vibration due to surface hydroxyls [**20-21**] These imply good hydrophilicity that is favorable to the photo catalytic activity of the nano-particles. According to Waldron [**22**] the band appeared at 598 cm^{-1}(υ_1) attributed to that of bending vibrations in tetrahedral complexes and at 425cm^{-1}(υ_2) is to the stretching vibration of Fe^{3+}–O^{2-} in the octahedral complexes [**23-24**].

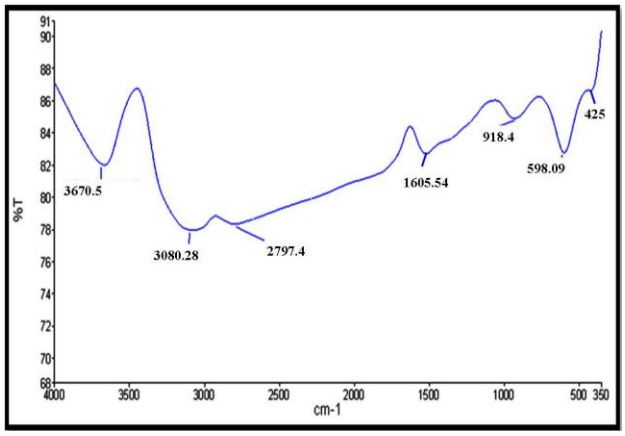

Fig. 1.4 Infrared spectra of $Co_{0.9}Mn_{0.1}Fe_2O_4$ nanoparticles.

Magnetic behavior of Mn doped cobalt ferrite nanoparticles is shown in **Fig. 1.5**.

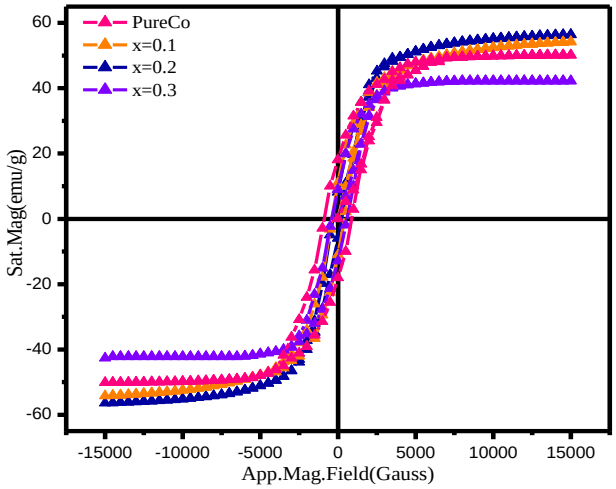

Fig. 1.5 Magnetic behavior of $Co_{1-x}Mn_xFe_2O_4$($0.0 \le x \le 0.3$).

In the present study an initial increase in the sat. mag.upto x=0.2 indicates initially at lower concentration of Mn the Mn^{2+} ion are substituted at the B(octa) site and at higher concentration (i.e.x=0.3), the rest of the Mn^{2+}ions are distributed at the A(tetra) site of the spinel lattice. The substitution of Mn^{2+} ($5\mu_B$)in place of Co^{2+}($3\mu_B$) also leads to increase value of Ms. Similar results are reported by Kim et.al.**[25].** The decrease in Hc (883 to 388 gauss) (**Table 1.1**)is attributed to decrease in octahedral Co^{2+} density due to Mn^{2+} substitution Similar magnetic properties of Mn doped cobalt ferrite Nps has been reported by previous researcher[**26**]. **Fig. 1.6** shows the varialtion of magnetic parameters with increasing Mn content. The magnetic moment per formula unit in Bohr magneton (μB) is calculated from following formula [**27**]:

$$n_B = \frac{M \times M_s}{5585} \quad \text{.....(5)}$$

where, M is molecular weight and Ms is saturation magnetization of respective samples.

For the cobalt ferrite, it is well known that Co^{2+} ions in the octahedral (B) sites are responsible for the origin of the anisotropy due to a strong spin-orbit interaction. The value of magnetic anisotropy constant (K_1) for the samples decreases with Mn^{2+} substitution. The observed behavior is attributed to the fact that Mn^{2+} replaces Co^{2+} ions in the B-sites, which is responsible for a high value of the anisotropy in cobalt ferrite**[28]**. The effective anisotropy constant (K_1) can be related to the saturation magnetization (Ms) and magnetic coercivity (Hc) as [**29**]:

$$H_c = \frac{K_1 \times 0.96}{M_s} \quad \text{.....(6)}$$

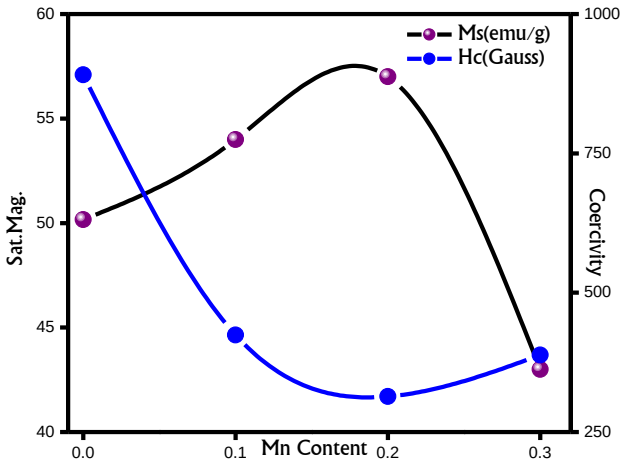

Fig. 1.6 variation of magnetic properties with increasing Mn concentration.

Conclusion

In this paper the structural and magnetic properties of CoMn ferrite nanoparticles annealed at 900ºC via co-precipitation route were investigated. The phase purity and crystalline nature was confirmed by XRD measurements. SEM images show ultrafine CoMn nanoparticles with uniform morphology. FTIR spectrum shows two absorption bands around 598 cm^{-1} and 425 cm^{-1} which represent intrinsic metal oxide stretching vibrations at tetrahedral and octahedral lattice sites. The change in magnetic properties of CoMn ferrite with increasing Mn content suggest that the obtained magnetic ferrites can be used for practical applications in recording media and magnetic data storage.

Acknowledgements

Author Swati Tapdiya acknowledge Jiwaji University to provide research opportunities, IUC Indore for XRD, IIT Roorkee for SEM and EDAX, IIT Chennai for VSM and ITM University Gwalior for FTIR facility for the completion of this research work.

Author's contributions

Conceived the plan: st,aks; Performed the expeirments: st; Data analysis: st, ss; Wrote the paper: st. Authors have no competing financial interests.

References

1. Valenzuela, R.; *Phys. Res. Int.*, **2012**, *591839*, 9. **DOI:**10.1155/2012/591839
2. Cheng, F.X.; Jia, J.T.; Xu, Z.G.; Zhou, B.; Liao, C.S.; Yan, C.H.; Chen, L.Y.; Zhao, H.B.; *J. Appl. Phys.*, **1999**, *86*, 2727. **DOI:**10.1063/1.371117
3. Yan, C.; Cheng, F.; Liao, C.S.; He, G.; *J. Magn.Magn. Mater*., **1999**, *192(3)*, 396. **DOI:**10.1016/S0304-8853(98)00549-6
4. Darshane, S.L.; Suryavanshi, S.S.; Mulla, I.S.; *Ceram. Int.*, **2009**, *35*, 1793. **DOI:**10.1016/j.ceramint.2008.10.013
5. Kamble, R.B.; Mathe, V.L.; *Sens. Actuators, B,***2008**, *131*, 205. **DOI**:10.1016/j.snb.2007.11.003
6. Kadam, A.; Shinde, S.S.; Yadav, S.P.; Rajpure, K.Y.; *J. Magn. Magn. Mater*.,2013, *329*, 59. **DOI:**10.1016/j.jmmm.2012.10.008
7. Ramana, C.V.; Kolekar, Y.D.; Kamala, B.K.; Sinha, B.; Ghosh, K.;*J. Appl. Phys.*, 2013, *114*, 183907. **DOI:**10.1063/1.4827416
8. Fannin, P.C.; Marin,C.N.; Malaescu, I.; Stefu, N.; Vlazan, P.; Novaconi, S.; Sfirloaga, P.; Popescu, S.; Couper, C.;*Mater. Des.*, 2011,*32*,1600. **DOI:**10.1016/j.matdes.2010.08.053
9. Zahi,S.;J.Electromagnetic Anal. Appl., 2010, *2*, 56. **DOI:**10.4236/jemaa.2010.21009
10. Dalawai, S.P.; Gadkari, A.B.;,Shinde, T.J.; Vasambekar, P.N.;*Adv. Mat. Lett*., 2013, *4*, 586. **DOI:**10.5185/amlett.2012.10431
11. Li, X.H.; Xu, C.L.; Han, X.H.;Qiao, L.; Wang, T.; Li, F.S.; Nanoscale, Res. Lett., 2010, *5*,1039. **DOI:**10.1007/s11671-010-9599-9
12. Nairan, A.; Khan, M.; Khan,U.; Iqbal, M.; Riaz, S. and Naseem, S.;Nanomaterials, 2016, *6*, 73. **DOI:**10.3390/nano6040073
13. Salunkhe, A.B.; Khot, V.M.; Thorat, N.D.; Phadatare, M.R.; Pawar, S.H.;Satish,C.I.; Dhawale, D.S.; *Appl. Surf. Sci.*, 2013, *264*, 598. **DOI:**10.1016/j.apsusc.2012.10.073
14. Tapdiya, S.; Shrivastava, A.K.; *Int. J. Innovative, Res. Sci. Eng. Technol.*, 2016, *5*, 6681. **DOI:**10.15680/IJIRSET.2016.0505011
15. Adeela, N.; Maaz, K.; Khan, U.; Karim, S.; Nisar, A.; Ahmad, M.; Ali, G.; Han, X.F.; Duan, J.L.; Liu, J.; *J. Alloy. Compd.*, 2015, *639*, 533. **DOI:**10.1016/j.jallcom.2015.03.203
16. Salunkhe, A.B.; Khot, V.M.; Phadatare, M.R.; Thorat, N.D.; Joshi, R.S.; Yadav, H.M.; Pawar, S.H.; *J. Magn. Magn. Mater*., 2014, *352*, 91. **DOI:**10.1016/j.jmmm.2013.09.020
17. Karimi, Z.; Mohammadifar, Y.; Shokrollahi, H.; Khameneh, S.H.; Yousefi, G.H.; Karimi, L.; *J. Magn. Magn. Mater.*, 2014, *361*, 150. **DOI:**10.1016/j.jmmm.2014.01.016
18. Yáñez-Vilar, S.; Sánchez-Andújar, M; Gómez-Aguirre, C.; Mira, J.; Señarís-Rodríguez, M.A.;Castro-García, S.; *J. Solid State Chem.*, 2009, *182(10)*, 2685. **DOI:**10.1016/j.jssc.2009.07.028
19. Lu, C.H.; Lou, S.J.; *Mater. Sci. Eng. B*, 2000, *75*, 38. **DOI:**10.1016/S0921-5107(00)00386-X
20. Priyadharsini, P.; Pradeep, A.; Sambasiva Rao, P.; Chandrasekaran, G.; *Mater. Chem. Phys*., 2009, *116*,207. **DOI:**10.1016/j.matchemphys.2009.03.011
21. Shen, X.C.; Fang, X.Z.; Zhou, Y.H.; Liang, H.; *Chem. Lett.*, 2004, *33*, 1468. **DOI:**10.1246/cl.2004.1468
22. Zhou, B.; Zhang, Y.W.; Liao, C.S.; Yan, C.H.; Chen, L.Y.; Wang, S.Y.; *J. Magn. Magn. Mater.*, 2004, *280*, 327. **DOI:**10.1016/j.jmmm.2004.03.031
23. Samoila, P.; Slatineanu, T.; Postolache, P.; Iordan, A.R.; Palamaru, M.N.; *Mater. Chem. Phys.*, 2012, *136*, 241. **DOI:**10.1016/j.matchemphys.2012.06.059
24. Zaki,H.M.; Dawoud,H.A.; *Physica B,* 2010, *405*, 4476. **DOI:**10.1016/j.physb.2010.08.018

25. Salunkhe, A.B.; Khot, V.M.; Phadatare, M.R.; Thorat, N.D.; Joshi, R.S.; Yadav, H.M.; Pawar, S.H.; *J. Magn. Magn. Mater*., 2014, *352*, 91.
DOI:10.1016/j.jmmm.2013.09.020
26. Roongtao, R.;Baitahe, R.; Vittayakorn,N.; Seeharaj,P.; Vittayakorn, W. C.;Ferroelectr., 2014, *459*, 119.
DOI:10.1080/00150193.2013.849175
27. Heiba, Z.K.; Mohamed, B. M.; Wahba, A.M.; Arda, L.; J Supercond Nov Magn., 2015, *28*, 2517.
DOI:10.1007/s10948-015-3069-7
28. Khan, U.; Adeela, N.; Javed, K.; Riaz, S.; Ali, H.; Iqbal, M.; Han, X.F.; Naseem, S.; *J. Nanopart. Res.*, **2015**, *17*, 429.
DOI:10.1007/s11051-015-3233-9
29. Bala, T.; Sankar, C.R.; Baidakova, M.; Osipov, V.; Enoki, T.; Joy, P.A.; Prasad, B.L.V.; Sastry, M.; *Langmuir*, **2005**, *21*, 10638.
DOI:10.1021/la051595k

